SAND2008-2674C

Nanoparticle Aerosols Form Knudsen Layers at Walls

J. R. Torczynski, M. A. Gallis, and D. J. Rader

Engineering Sciences Center, Sandia National Laboratories, P. O. Box 5800, Albuquerque, NM 87185-0346, USA

Abstract. An aerosol of nanoparticles forms a Knudsen layer when diffusing in a Brownian fashion toward a solid wall. More specifically, the particle number density in the gas by the wall approaches a nonzero value proportional to the flux. An approximate theory for the coefficient of proportionality as a function of the particle sticking probability at the wall and the drift velocity normal to the wall is compared to Langevin particle simulations. The results are used to formulate a boundary condition that enables accurate advection-diffusion simulations of nanoparticle-aerosol transport.

Keywords: nanoparticles, aerosol, wall concentration, boundary condition, advection-diffusion, transport modeling
PACS: 05.40.Jc, 51.20.+d, 81.07.Wx, 85.85.+j

INTRODUCTION

In theoretical treatments of aerosol transport, the particle number density in the gas adjacent to a solid wall is almost universally considered to be zero [1]. While an excellent approximation for micron-scale aerosol particles in ambient air, this assumption breaks down for atmospheric aerosols of nanoparticles now used in experiments [2]. Rather than vanishing at a wall, the particle number density approaches a nonzero value proportional to the particle flux to the wall even when the probability that an impacting particle sticks is unity. The presence of the wall modifies the particle velocity distribution function from its form in an unbounded medium within a few thermal stopping distances of the wall. This affected region is denoted here as the "particle Knudsen layer" by analogy to the Knudsen layer observed for gas molecules within a few mean free paths of a wall [3]. The particle Knudsen layer is investigated theoretically using the generalized Fokker-Planck equation [4] and computationally via massively parallel particle-transport simulations based on the Langevin equation for Brownian particle motion [5].

Two idealized reflection processes are investigated that include the important physics but avoid the complexity of real particle-wall interactions [6,7]. In the first, a velocity-independent sticking fraction is prescribed, and any particle impacting the wall has this probability of sticking regardless of its incident velocity. In the second, a cutoff velocity is prescribed, and any particle impacting the wall sticks if its normal incident velocity is less than this value. In both processes, if a particle does not stick, the reflection is taken to be specular.

GENERALIZED FOKKER-PLANCK APPROXIMATION

An approximate theory for the behavior of particles near a wall is developed for these two reflection processes. For a nonzero flux to the wall, the particle velocity distribution in the gas far from the wall is applied at the wall, and the outgoing portion of the flux is equated to the reflected part of the incoming portion of the flux.

Chandrasekhar [4] derives the generalized Fokker-Planck equation (GFPE) for the dynamics of a particle in a fluid, Equation (249) of his treatise, given below in slightly different notation:

$$\frac{\partial N}{\partial t} + \frac{\partial}{\partial \mathbf{x}} \cdot \left(\mathbf{u} N \right) + \frac{1}{\tau} \frac{\partial}{\partial \mathbf{u}} \cdot \left(-\mathbf{v} N \right) = \frac{c^2}{2\tau} \frac{\partial}{\partial \mathbf{u}} \cdot \left(\frac{\partial N}{\partial \mathbf{u}} \right). \tag{1}$$

Here, N is the particle velocity distribution function, t is time, $\mathbf{x}$ is position, $\mathbf{u}$ is particle velocity, $\mathbf{v} = \mathbf{u} - \mathbf{U}$ is particle thermal velocity, $c = \left(2 k_B T / m \right)^{1/2}$ is the most probable particle thermal speed when N is a Maxwellian distribution at temperature T, k_B is the Boltzmann constant, $m = \pi d^3 \varsigma / 6$ is the particle mass, d is the particle

diameter, ς is the particle mass density, $\mathbf{U} = \mathbf{F}/\beta$ is the drift velocity, $\mathbf{F}$ is the total non-drag force on a particle (e.g., $\mathbf{F} = m\mathbf{g}$ is the force from a gravitational acceleration of $\mathbf{g}$), $\tau = m/\beta$ is the particle stopping time, β is the particle drag coefficient (force per unit velocity), and $D = c^2\tau/2 = k_B T/\beta$ is the Stokes-Einstein particle diffusivity [1]. Herein, all particle and gas parameters are taken to be independent of time and position, and the gas is taken to be motionless. For this situation, the above equation has the following time-independent solution:

$$N = \frac{\tilde{n}}{\pi^{3/2}c^3}\exp\left[-\frac{\mathbf{v}\cdot\mathbf{v}}{c^2}\right],\ \tilde{n} = n_\infty + n_1\exp\left[\frac{2\mathbf{U}\cdot(\mathbf{x}-\tau\mathbf{v})}{c^2\tau} - \frac{\mathbf{U}\cdot\mathbf{U}}{c^2}\right] \to n_0 + \left(\frac{\partial n}{\partial \mathbf{x}}\right)_0 \cdot(\mathbf{x}-\tau\mathbf{v}). \tag{2}$$

Here, n denotes particle number density, subscripts indicate quantities that are independent of time and position, and the arrow denotes the zero-drift-velocity limit ($\mathbf{U} \to \mathbf{0}$). The zero-drift-velocity solution is physically realizable only in the limit of a small particle-number-density gradient, which ensures that regions of negative probability density occur only at large velocities and thus are exponentially small.

Under well-understood circumstances [1], aerosol transport is described by the advection-diffusion equation:

$$\frac{\partial n}{\partial t} + \frac{\partial}{\partial \mathbf{x}}\cdot\left(n\mathbf{U} - D\frac{\partial n}{\partial \mathbf{x}}\right) = 0 \text{ in the gas.} \tag{3}$$

At a wall, the advection-diffusion equation requires a boundary condition, which is almost universally taken to be the zero-concentration condition: $n = 0$ at the wall [1].

Although it is strictly applicable only in unbounded space, the GFPE solution can be used to construct a more general boundary condition for the advection-diffusion equation. This boundary condition has the following form, where f is termed the "particle-flux coefficient" and $\hat{\mathbf{n}}$ is the unit normal pointing into the wall and out of the gas:

$$\hat{\mathbf{n}}\cdot\left(n\mathbf{U} - D\frac{\partial n}{\partial \mathbf{x}}\right) = \frac{nc}{\pi^{1/2}}f \text{ at the wall.} \tag{4}$$

This "particle-flux boundary condition" is exactly analogous to the well-known velocity-slip and temperature-jump boundary conditions [3], in which discontinuities in tangential velocity and temperature between a wall and the adjacent gas are proportional to shear stress and heat flux, respectively. The particle-flux boundary condition is found by applying the GFPE solution for unbounded space at the wall, equating the outgoing portion of the flux to the reflected amount of the incoming portion of the flux, where $R[\mathbf{u}]$ represents the reflection probability,

$$\int_{-\hat{\mathbf{n}}\cdot\mathbf{u}>0} N(-\hat{\mathbf{n}}\cdot\mathbf{u})\,d\mathbf{u} = \int_{\hat{\mathbf{n}}\cdot\mathbf{u}>0} R[\mathbf{u}]N(\hat{\mathbf{n}}\cdot\mathbf{u})\,d\mathbf{u}, \tag{5}$$

and rearranging the resulting expression into the form of Equation (4). This approach is applied to the two reflection processes discussed above. The sticking-fraction process has $R[\mathbf{u}] = 1 - s$ and yields the below expression, where $U = \mathbf{U}\cdot\hat{\mathbf{n}}$ is the normal drift velocity (positive into the wall) and $\hat{U} = U/c$ is its normalized value:

$$f = s\left\{2 - s\left(1 + \operatorname{erf}\left[\hat{U}\right] - \left\{\left(1 - \exp\left[-\hat{U}^2\right]\right)\Big/\left(\pi^{1/2}\hat{U}\right)\right\}\right)\right\}^{-1}. \tag{6}$$

The cutoff-velocity process has $R[\mathbf{u}] = \mathrm{H}[\hat{\mathbf{n}}\cdot\hat{\mathbf{u}} - \hat{U}_n]$ and yields the below expression, where H is the Heaviside function, U_n is the cutoff velocity, $\hat{U}_n = U_n/c$ is its normalized value, and $\hat{U}_d = \hat{U}_n - \hat{U}$:

$$f = \left\{\pi^{1/2}\hat{U}\left(1 - \exp\left[-\hat{U}_n^2\right]\right)\right\}\Big/\left\{1 - \exp\left[-\hat{U}_n^2\right] - \exp\left[-\hat{U}^2\right] + \exp\left[-\hat{U}_d^2\right] + \pi^{1/2}\hat{U}\left(\operatorname{erfc}\left[\hat{U}_d\right] + \operatorname{erfc}\left[\hat{U}\right]\right)\right\}. \tag{7}$$

It is convenient to characterize the cutoff-velocity reflection process using the "cutoff parameter" $\sigma = 1 - \exp[-\hat{U}_n^2]$ in place of the normalized cutoff velocity $\hat{U}_n$. The cutoff parameter σ is similar to sticking fraction s in that $\sigma = 1$

($\hat{U}_n \to \infty$) and $s = 1$ both correspond to all particles sticking and $\sigma = 0$ ($\hat{U}_n = 0$) and $s = 0$ both correspond to all particles reflecting. For an incident half-range Maxwellian, the cutoff parameter equals the sticking fraction; however, when the flux to the wall is nonzero, the incident distribution is not a half-range Maxwellian.

LANGEVIN PARTICLE SIMULATIONS

Simulations are performed for particles in a gas near a wall. The gas is taken to be a thermal bath at temperature T, so its molecules are not directly simulated. The stochastic motion of a particle of mass m at position $\mathbf{x}$ with velocity $\mathbf{u}$ is described by the Langevin equation [5] with particle drag coefficient β, constant drift velocity $\mathbf{U}$, and random thermal force $\mathbf{X}$ corresponding to the gas conditions at temperature T:

$$m\,d\mathbf{u}/dt = \beta\left(\mathbf{U}-\mathbf{u}\right)+\mathbf{X},\ d\mathbf{x}/dt = \mathbf{u}. \tag{8}$$

Ermak and Buckholz [5] present an algorithm for integrating the Langevin equation forward in time based on the GFPE solution of Chandrasekhar [4] for the distribution function of a particle with velocity $\mathbf{u}_0$ and position $\mathbf{x}_0$ at time t_0. More specifically, they present a method of selecting two independent Gaussian random vectors $\mathbf{B}_1$ and $\mathbf{B}_2$ to advance the particle velocity and position from $\mathbf{u}_0$ and $\mathbf{x}_0$ at time t to $\mathbf{u}$ and $\mathbf{x}$ at time $t+\Delta t$:

$$\mathbf{u} = \mathbf{u}_0\delta + \mathbf{U}\left(1-\delta\right)+\mathbf{B}_1,\ \mathbf{x} = \mathbf{x}_0+\tau\left(\mathbf{u}+\mathbf{u}_0-2\mathbf{U}\right)\left\{\left(1-\delta\right)/\left(1+\delta\right)\right\}+\mathbf{U}\Delta t+\mathbf{B}_2,\ \delta = \exp\left[-\Delta t/\tau\right];$$
$$\left\langle\mathbf{B}_1\right\rangle = \mathbf{0},\ \left\langle\mathbf{B}_2\right\rangle = \mathbf{0},\ \left\langle\mathbf{B}_1\cdot\mathbf{B}_2\right\rangle = 0,\ \left\langle\mathbf{B}_1\cdot\mathbf{B}_1\right\rangle = \left(3/2\right)c^2\left(1-\delta^2\right),\ \left\langle\mathbf{B}_2\cdot\mathbf{B}_2\right\rangle = 3c^2\tau^2\left\{\left(\Delta t/\tau\right)-2\left(1-\delta\right)/\left(1+\delta\right)\right\}. \tag{9}$$

The Ermak-Buckholz algorithm is implemented in an existing Direct Simulation Monte Carlo (DSMC) code [8]. This approach takes advantage of the similarity between tracking particles and molecules: the only significant difference is that particles interact with a background fluid whereas molecules collide with one another. Moreover, the particle-tracking implementation is massively parallel, with good scaling behavior through 10,000 processors, and is therefore capable of simulating billions of particles simultaneously [8,9,10,11].

TABLE 1. Physical and numerical parameters used in analysis and simulation: air and polystyrene latex (PSL).

Boltzmann constant	k_B	1.380658×10^{-23} J/K	Slip parameter, particle	α_s	1.165
Molecular mass, gas	M	4.811×10^{-26} kg	Slip parameter, particle	β_s	0.483
Pressure, gas	p	101325 Pa	Slip parameter, particle	γ_s	0.997
Temperature, gas	T	300 K	Drag coefficient, particle	β	2.950×10^{-13} N/(m/s)
Mass density, gas	ρ	1.177 kg/m^3	Stopping time, particle	τ	14.91 ns
Molecular mean speed, gas	$\bar{c}$	468.2 m/s	Thermal speed scale, particle	c	1.3724 m/s
Viscosity, gas	μ	1.85×10^{-5} Pa·s	Diffusivity, particle	D	1.404×10^{-8} m^2/s
Hard-sphere parameter, gas	ϕ	$5\pi/32 \approx 0.491$	Stopping distance, particle	ℓ	18.13 nm
Mean free path, gas	λ	68.37 nm	Domain length	L	1000 nm
Diameter, particle	d	20 nm	Cell size	Δx	4 nm
Mass density, particle	ς	1050 kg/m^3	Time step	Δt	0.5 ns
Mass, particle	m	4.398×10^{-21} kg	Steady-state time	t_L	10^6 ns
Knudsen number, particle	Kn	6.837	Gravitational acceleration	g	0 m/s^2

Table 1 shows the gas and particle parameters for the Langevin simulations. Spherical polystyrene latex (PSL) particles of diameter $d = 20$ nm and ambient air are considered, as in recent experiments [2]. The molecular mean free path is $\lambda = \mu/\phi\rho\bar{c}$, where μ is the gas viscosity, $\phi = 5\pi/32$ is a constant, $\rho = Mp/k_BT$ is the gas mass density, $\bar{c} = \left(8k_BT/\pi M\right)^{1/2}$ is the molecular mean speed, and M is the molecular mass. The particle Knudsen number is $\mathrm{Kn} = 2\lambda/d = 6.837$, and the drag coefficient is $\beta = 3\pi\mu d/C$, where the numerator is Stokes drag and the denominator is a slip correction factor of the form $C = 1+\mathrm{Kn}\left(\alpha_s+\beta_s\exp\left[-\gamma_s/\mathrm{Kn}\right]\right)$ [1,2]. For these conditions, the particle thermal stopping distance is $\ell = \pi^{1/2}D/c = \left(\pi^{1/2}/2\right)c\tau = 18.13$ nm, which is similar to the particle diameter.

Table 1 also shows the numerical parameters used in these simulations. The wall is located at $x = 0$, and the particle source is located at $x = L$, where $L = 1000$ nm. This domain is divided into 250 cells of width $\Delta x = 4$ nm. Initially, the domain is devoid of particles. Particles enter the domain at a fixed rate from the source (particles

attempting to exit are reflected specularly), and particles interact with the wall according to one of the reflection processes. Time steps of $\Delta t = 0.5$ ns are used, and a time of $t_L = 10^6$ ns is allowed to pass before sampling is initiated to ensure that steady behavior is established. Typical simulations use $\sim 10^5$ particles in the domain and sample $\sim 10^9$ particles per cell over $\sim 10^7$ time steps of steady behavior. Simulations typically require 96 hours on 200 processors of a Linux cluster (i.e., about 2 processor-years).

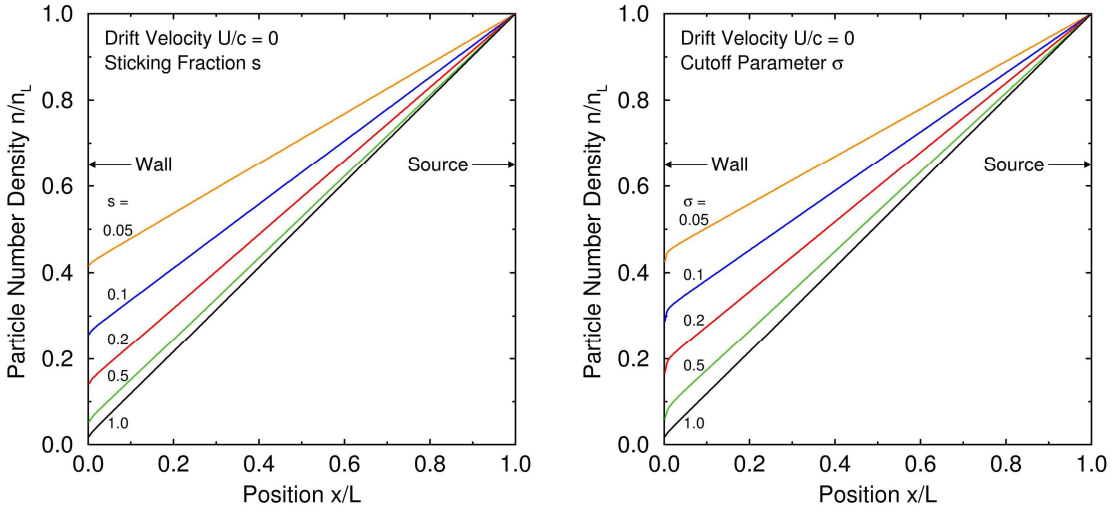

FIGURE 1. Particle-number-density profiles for two wall interactions: left, sticking fraction; right, cutoff velocity.

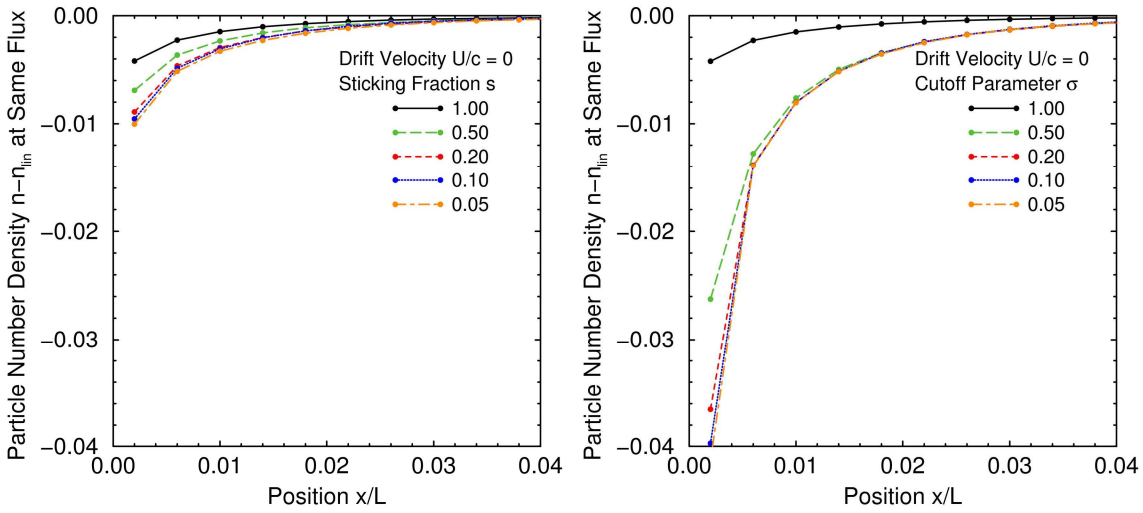

FIGURE 2. Particle-number-density Knudsen layers (departure from linearity): left, sticking fraction; right, cutoff velocity.

Figure 1 shows particle-number-density profiles from Langevin simulations for both reflection processes with a zero drift velocity. The profiles are normalized so that the particle number density is unity at the source ($x = L$). Profiles are shown for five values of the sticking fraction s (left plot) and the cutoff parameter σ (right plot): 0.05, 0.1, 0.2, 0.5, and 1.0. Each cutoff-velocity profile lies slightly above the corresponding sticking-fraction profile except for the case of $s = \sigma = 1$, for which the two profiles are identical to within the precision of the simulations. All profiles vary linearly with position except near the wall. This near-wall region, located roughly within $0 \le x/L < 0.1$ (i.e., $0 \le x < 100$ nm, $0 \le x/\ell < 5$), contains the particle Knudsen layer of each profile. The particle number density adjacent to the wall is nonzero for all profiles.

Figure 2 shows the near-wall Knudsen layers for the profiles in Figure 1. Each Knudsen layer is determined by taking the difference between the actual profile $n[x]$ and a straight-line fit $n_{\text{lin}}[x]$ through its linear portion away from the wall and subsequently dividing this difference by the slope of the straight-line fit. This slope scaling is

performed so that all Knudsen layers are shown at the same particle flux. In all cases except $s = \sigma = 1$, the departure of the Knudsen layer from the corresponding straight-line fit is larger for the cutoff-velocity reflection process than for the sticking-fraction reflection process, and the departure increases as the sticking fraction or the cutoff parameter is decreased (i.e., as more particles are reflected by the wall).

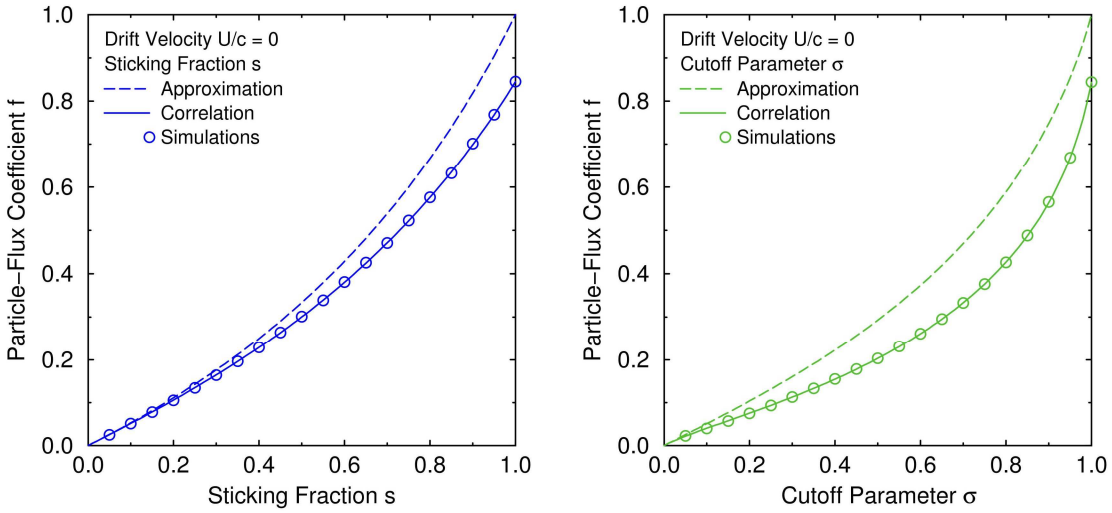

FIGURE 3. Particle-flux coefficient at zero drift velocity for two wall interactions: left, sticking fraction; right, cutoff velocity.

COMPARISON

Figure 3 shows the particle-flux coefficient f as a function of the sticking fraction s (left plot) and the cutoff parameter σ (right plot) for zero drift velocity. The particle-flux coefficient is determined as follows. The straight-line fit yields a slope of $(dn/dx)_0$ and an intercept of n_0 at $x = 0$. The particle-flux coefficient is then found from the particle-flux boundary condition (Equation (4)): $f = (\pi^{1/2} D/cn_0)(dn/dx)_0$. The symbols are the simulation values, the dashed curves are the GFPE approximations ((Equations (6) and (7)), and the solid curves are empirically determined correlations that represent the simulation values to ±0.001 (their uncertainty):

$$f = \left(\frac{s}{2-s}\right)\left(\frac{1+0.506s}{1+0.783s}\right), \text{ sticking fraction; } f = \frac{0.5\sigma + 1.665\sigma^2 - 1.843\sigma^3}{1 + 7.412\sigma - 12.456\sigma^2 + 4.426\sigma^3}, \text{ cutoff velocity.} \tag{10}$$

The differences between the approximation and simulation values are modest for the sticking-fraction reflection process but are larger for the cutoff-velocity reflection process. This is not surprising because, for the cutoff-velocity reflection process, the reflected part of the incoming portion of the particle velocity distribution differs substantially in shape from the outgoing portion.

Figure 4 (left plot) shows profiles of the particle number density when the drift velocity is nonzero. In these cases, the profiles decay exponentially in the upstream direction of the drift velocity. Figure 4 (right plot) also shows the particle-flux coefficient f as a function of the normalized drift velocity $\hat{U} = U/c$ when all particles stick to the wall ($s = \sigma = 1$). The symbols represent the simulation results, the dashed curve represents the GFPE approximation (Equation (6)) with $s = 1$, and the dotted curves represent the asymptotic behavior of the approximation for large positive or negative values of the drift velocity. The differences between the simulation and approximation values are modest and comparable to those observed in the preceding figure.

CONCLUSIONS

This theoretical and numerical investigation demonstrates that the particle number density of an aerosol tends to a nonzero value at a wall and that this value is proportional to the flux and depends upon the reflection process. This effect is important for standard nanoparticles now available for experimentation and becomes more important as the

probability that an incident particle sticks to the wall is reduced. A methodology is developed that enables an approximate advection-diffusion boundary condition to be determined for arbitrary reflection processes. Although developed for a flat surface, this boundary condition can be used for a nonflat surface so long as its radius of curvature is large compared to the thickness of the particle Knudsen layer (corners do not satisfy this restriction).

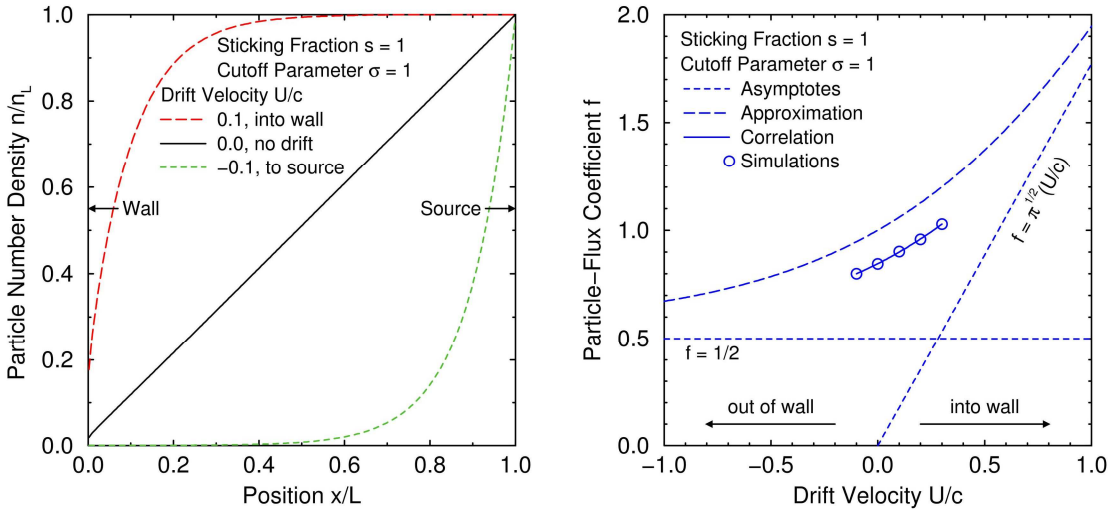

FIGURE 4. Left: particle-number-density profiles with nonzero drift velocity. Right: corresponding particle-flux coefficients.

ACKNOWLEDGMENTS

Sandia is a multiprogram laboratory operated by Sandia Corporation, a Lockheed Martin Company, for the United States Department of Energy's National Nuclear Security Administration under contract DE-AC04-94AL85000. The authors gratefully acknowledge financial support from Intel Corporation under CRADA SC93/01154 and technical interactions with Kevin J. Orvek, Intel contract monitor, David Y. H. Pui and Jing Wang, University of Minnesota, and Christof Asbach and Heinz Fissan, IUTA, Deutschland.

REFERENCES

1. S. K. Friedlander, *Smoke, Dust, and Haze: Fundamentals of Aerosol Dynamics*, New York: Oxford, 2000.
2. J. H. Kim, G. W. Mulholland, S. R. Kukuck, and D. Y. H. Pui, "Slip Correction Measurements of Certified PSL Nanoparticles Using a Nanometer Differential Mobility Analyzer (Nano-DMA) for Knudsen Number from 0.5 to 83," *Journal of Research of the National Institute of Standards and Technology*, **110** (1), 31-54 (2005).
3. G. A. Bird, *Molecular Gas Dynamics and the Direct Simulation of Gas Flows*, Oxford: Clarendon, 1994.
4. S. Chandrasekhar, "Stochastic Problems in Physics and Astronomy," *Reviews of Modern Physics*, **15** (1), 1-89 (1943).
5. D. L. Ermak and H. Buckholz, "Numerical Integration of the Langevin Equation: Monte Carlo Simulation," *Journal of Computational Physics*, **35** (2), 169-182 (1980).
6. J. Happel and H. Brenner, *Low Reynolds Number Hydrodynamics*, The Hague: Martinus Nijhoff, 1983.
7. B. Dahneke, "The Capture of Aerosol Particles by Surfaces," *Journal of Colloid and Interface Science*, **37** (2), 342-353 (1971).
8. M. A. Gallis, D. J. Rader, and J. R. Torczynski, "DSMC Simulations of Brownian Dynamics of Particles," paper AIAA 2002-2760, American Institute of Aeronautics and Astronautics, Reston, 2002.
9. M. A. Gallis, J. R. Torczynski, and D. J. Rader, "Nanoparticle Knudsen Layers in Gas-Filled Microscale Geometries," *Physical Review E*, **77**, 036302/1-7 (2008).
10. J. R. Torczynski, M. A. Gallis, and D. J. Rader, "Particle-Contamination Analysis for Reticles in Carrier Inner Pods," *Proceedings of SPIE*, **6921**, 69213G/1-11 (2008).
11. M. A. Gallis, J. R. Torczynski, and D. J. Rader, "Nonzero-Concentration Boundary Condition for Advection-Diffusion Aerosol-Transport Modeling," *Aerosol Science and Technology*, submitted (2008).